H-induced structural phase transitions on W(100) by surface infrared spectroscopy

J. J. Arrecis,* Y. J. Chabal, and S. B. Christman
AT&T Bell Laboratories, Murray Hill, New Jersey 07974
(Received 22 January 1986)

A vibrational study of the various H-induced phases on W(100) at room temperature has been carried out using surface infrared spectroscopy. A large shift ($\gtrsim 35$ cm^{-1}) in the frequency of the W_2H symmetric stretch mode, ν_1, is observed at low coverages ($\Theta \leq 0.3$), indicating a local structural rearrangement (≈ 0.03 Å) of the W atoms as the commensurate $(\sqrt{2}\times\sqrt{2})R45°$ phase is established at $\Theta = 0.3$. The incommensurate phase, I-$(\sqrt{2}\times\sqrt{2})$, is made up of reconstructed domains ($\nu_1 \approx 1300$ cm^{-1}) separated by domain walls of *finite size* and with unreconstructed W atoms as evidenced by a new H vibration at ≈ 1100 cm^{-1}. As the coverage is increased ($\Theta > 0.5$), the reconstructed domains decrease in size with a substantial expansion of the W dimer and finally disappear ($\Theta \approx 1$). The disordered surface that ensues is brought back into registry with the bulk at saturation ($\Theta = 2$).

I. INTRODUCTION

There is now a large body of evidence which indicates that the H-induced phases on the W(100) surface[1] involve structural rearrangement of the substrate surface atoms. It was first the occurrence of displacive phase transition on the *clean* W(100) surface[2-7] which suggested that the presence of H may stabilize some phases characterized by a well-defined W reconstruction.[8,9] These hypotheses were later confirmed by high-energy ion scattering-channeling experiments which clearly demonstrated that the H-induced phases at low coverage are reconstructed.[10,11] Furthermore, large changes in vibrational frequency of H on W(100) as a function of coverage could be accounted for by large tungsten displacements at low H coverage.[12]

The main phases are the "commensurate" $(\sqrt{2}\times\sqrt{2})R45°$ phase ($\Theta \approx 0.3$, always in units of monolayers in the present work), characterized by a sharp $(\frac{1}{2},\frac{1}{2})$ spot, the "incommensurate," I-$(\sqrt{2}\times\sqrt{2})$ phase ($0.3 < \Theta < 0.5$) characterized by a split $(\frac{1}{2},\frac{1}{2})$ spot, the "disordered" phase ($0.6 < \Theta < 1.9$), and the "ordered" phase at saturation ($\Theta = 2$).[1] The transitions between these phases are reversible[13,14] and the critical coverages depend on temperature.[15,16] While it is now believed that the clean surface reconstruction, involving displacements of the top W atoms along the $\langle 11 \rangle$ direction is driven by a strong coupling of the W motion to surface electronic states,[17-22] the H-induced reconstructions are not as well understood. The short-range nature of electronic interactions have motivated lattice-dynamical models[23] which have shown that purely *short-range,* nearest- and next-nearest-neighbor, W-W interactions can produce the observed phases. For the H-covered surface, Ying *et al.*[24-28] and Inaoka *et al.*[29] have been able to account for most of the observed phases by focusing on the structural aspects of the transitions.

If a short-range Jahn-Teller–like mechanism dominates, then it is particularly important to probe the short-range, local arrangement of the surface and to correlate such results to the long-range order determined by low-energy electron diffraction (LEED) studies. While direct electronic measurements, such as ultraviolet photoemission (UPS), have been instrumental in understanding the *clean* surface phase transitions,[17,18,30-36] they have so far failed to provide the detailed local picture of the H-induced phases.

Vibrational spectroscopy is one of the best candidates to probe the local arrangement of the surface around the adsorbed H atoms. Indeed, after first establishing the atomic nature of hydrogen on W(100),[37] electron energy-loss spectroscopy (EELS) data were key in determining the bridge adsorption site for all coverages.[12,38] Detailed analyses[39,40] have made it possible to derive atomic positions in the vicinity of the hydrogen, in particular confirming a "pinched" and "relaxed" W atom position at low and high coverages, respectively. However, especially in view of more recent EELS data,[41] it is clear that higher resolution is required to unravel the subtle changes (e.g., in peak positions or line shapes) occurring during the transitions. A quantitative monitoring of these changes is critical for further theoretical modeling.

This paper presents infrared absorption data obtained for hydrogen coverages between $\Theta = 0.04$ and $\Theta = 2$ (saturation) at room temperature. This range encompasses the $(\sqrt{2}\times\sqrt{2})R45°$ phases before and after the symmetry switching, the commensurate (C) and incommensurate (I)-$(\sqrt{2}\times\sqrt{2})R45°$ phases, the disordered phase and the ordered saturated phase. The information which is particularly important for the understanding of the phase transitions *and* which was *not available* from previous EELS studies is the H-vibrational spectrum at the lowest coverages ($\Theta = 0.04$ to $\Theta = 0.3$) and the spectrum variations in the $C \rightarrow I$-$(\sqrt{2}\times\sqrt{2})$ transition region.

In Sec. II, the experimental apparatus is described with emphasis on the *simultaneous* LEED and ir measurements capabilities for the low-coverage data. In Sec. III, the LEED results are summarized in order to calibrate our data with the results of other laboratories and to define the phases of interest. In Sec. IV, the ir data are presented

as a function of coverage and details of the H coverage calibration are given. In Sec. V, our results are discussed in view of the various theoretical models proposed so far. Section VI summarizes the main conclusions drawn from the ir data.

II. EXPERIMENTAL

The experimental apparatus is comprised of a modified Nicolet 6000 infrared interferometer and an ultrahigh-vacuum chamber.[42] Reflective optics, CsI windows, and a broadband Hg-Cd-Te detector make it possible to study the region from 600 to 4000 cm^{-1} with reasonable signal-to-noise ratio (S/N). In particular, changes in reflectivity, $\Delta R/R \lesssim 10^{-4}$ with a 4-cm^{-1} resolution, can be measured in a few minutes from 700 to 1500 cm^{-1}, i.e., over the range relevant for infrared active W_2H and W_2D vibrations.

The W(100) crystal (2.5 cm$\times$0.75 cm$\times$0.13 cm) faces the LEED screen during the ir reflection experiment (one bounce, 85° incidence angle). It was grown, oriented ($\pm 0.5°$), spark cut, and polished by the Material Research Center at Cornell University. Apart from some rounding of about 1 mm at the edges, the rest of the surface is mirror like.

Prior to any measurements, the W sample was cleaned by repeated baking at 1475 K in 10^{-7} Torr of O_2 ($\gtrsim$10 h) and flashing in vacuum to 2150 K. After most of the carbon originating from the bulk had been removed, cleaning was performed by high-temperature flashes only (pressure rise less than 3×10^{-10} Torr), prior to each individual run. The Auger spectra obtained with a single-pass cylindrical mirror analyzer (CMA) showed that less than 1% monolayer of carbon and oxygen were present following the ir-LEED measurements ($\gtrsim \frac{1}{2}$ h) at the working pressure of 3×10^{-11} Torr. The LEED patterns, e.g., the low-temperature $(\sqrt{2}\times\sqrt{2})R45°$ showed no measurable variation as the sample was translated in front of the LEED beam.

The sample temperature was measured with a WRe 5%-WRe 26% thermocouple spot welded to the bottom edge of the sample. The H_2, D_2 leak values were located close to the Bayard-Alpert gauge ($\approx$5 cm) but far from the sample ($\approx$30 cm) without a direct line of sight. In addition, the leak valves faced the cold shroud of a Ti-sublimator pump. As a result, the exposures quoted in this paper (determined from the gauge reading, corrected for H_2) are slightly higher (10–20 %) than the actual exposures on the sample surface. The mass spectrometer was not located in direct line of sight of the sample so that flash desorption could not be used as an *accurate* means to determine the coverage.

The H-induced spectra were obtained by ratioing the reflection spectra of the H-covered surface to those of the clean W(100) surface. From a practical point of view, however, the order in which the respective spectra were taken was important. The sample was first cleaned by a high-temperature electron bombardment flash. After about 15 min after the flash the sample had cooled down to room temperature and the signal was stable, i.e., the ratio of two consecutive ir runs ($\approx$3 min) was flat over all the frequency range accessible and the noise level was less than 10^{-4} of the total signal. Only then was H_2 introduced to achieve a given coverage and two spectra were taken. Further exposures could then be repeated to produce higher coverages and the new spectra ratioed to the original clean sample spectrum. The base pressure was such ($\approx 2\times10^{-11}$ Torr) that the sample remained clean for about 1 h after the high-temperature flash, after which no data were ever taken. The above procedure minimized the noise arising from thermal drifts in the sample manipulator.

The clean W(100) surface and the various H-covered surfaces have different W rearrangement (reconstruction). As a result, the conduction electron scattering from the surface varies with H-coverage, i.e., W reconstruction.[43] These variations are reflected in broadband reflectivity changes which can be distinguished from purely vibrational absorption by detailed comparison of the H- and D-induced spectra taken at *identical* coverages.

The LEED measurements were performed using a rear-view LEED arrangement. For routine records, a standard camera was used to take pictures. For studying the subtle changes in spot intensity at very low coverages ($\Theta=0.04$ to 0.3), the standard camera was replaced by an optical multichannel analyzer (OMA) (EG&G PAR, Model III) equipped with a silicon intensified target (SIT) camera. The two-dimensional data were digitized and the area under each diffraction feature could be integrated numerically.

No work-function probe was available at the time of the experiments. As a result, an absolute coverage determination could not be performed. All the coverages quoted in this paper are obtained assuming that, at saturation, $\Theta=2\times10^{15}$ H atoms/cm^2, i.e., 2 H per W atom, and following the procedure detailed in Sec. IV E.

III. RESULTS: LEED

Figure 1 summarizes the main LEED patterns observed as a function of H coverage. In agreement with previous work[1,5–9] we find that the $(\frac{1}{2},\frac{1}{2})$ LEED spot indicated by an arrow for $\Theta<0.5$ sharpens with H coverage up to $\Theta\approx0.30$. The sharpening has been interpreted as resulting from the development of large size domains with $(\sqrt{2}\times\sqrt{2})R45°$ symmetry as shown in Fig. 2(b). From $\Theta=0.33$ to $\Theta=0.42$, as calibrated according to Sec. IV E, the $(\frac{1}{2},\frac{1}{2})$ spot splits into four spots, indicated a modulation of the domains. The split phase is called incommensurate, I-$(\sqrt{2}\times\sqrt{2})$, and is believed to involve (on flat samples) the two possible orientations of regions with antiphase domain structures within each region.[15]

The spots begin to streak (see $\Theta=0.48$) in a perpendicular direction to the splitting axis after the splitting becomes $\frac{1}{4}$ of the (1×1) unit cell. This indicates a loss of long-range order in a direction normal to that of the modulation. Finally, faint $\frac{1}{5}$ order spots appear in the range of $\Theta=0.9$ (see arrow for $\Theta=0.88$) before a 1×1 pattern is established for $\Theta>1$.

The low-coverage range was investigated more quantitatively by measuring the integrated intensity of the $(\frac{1}{2},\frac{1}{2})$ spot by means of the OMA camera. The results

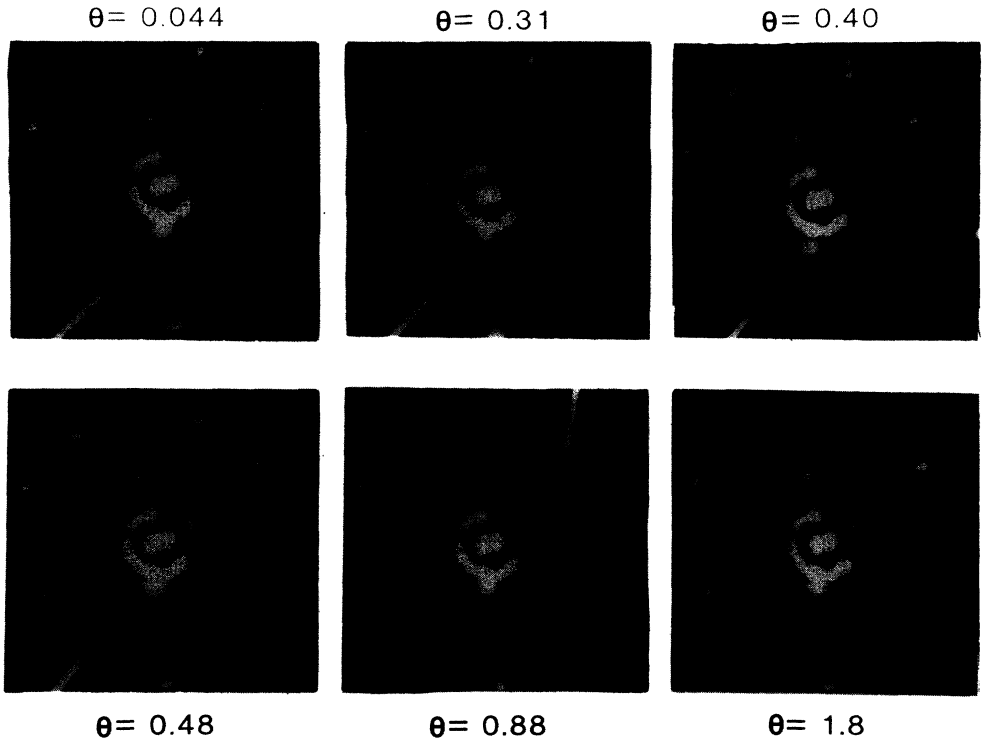

FIG. 1. Summary of the main stages of reconstruction as a function of coverage as monitored by LEED. For $\Theta=0.04$, 0.31, 0.40, and 0.48, the $(\frac{1}{2},\frac{1}{2})$ LEED spot is indicated by an arrow. The coverage is determined by ir absorbance and exposure (see Sec. IV E). For $\Theta\approx 0.88$, the weak $\frac{1}{5}$-order spot is marked. The coverages for the last two frames are estimated using ir absorbance and interpolation between $\Theta=0.6$ and $\Theta=2$.

are shown in Fig. 3. The intensity features an approximately linear rise with coverage below $\Theta\approx 0.3$ except for a small dip around $\Theta=0.16$. Such a dip has been previously reported by Griffiths *et al.*[44] and found to correlate with the long-range symmetry switching of the W atoms from a ⟨11⟩ reconstruction [Fig. 2(a)] to a ⟨10⟩ reconstruction [Fig. 2(b)]. Note, however, that because of dif-

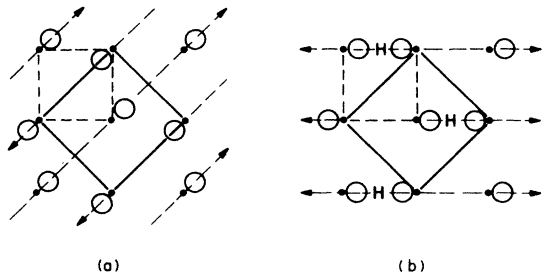

FIG. 2. Reconstructions of the W(100) surface. The open circles represent the displaced W atoms and the solid dots the position of the W atoms if no reconstructions occurred. (a) Reconstruction associated with the clean W(100) surface at or below room temperature. The light dashed lines (with arrow) indicate the direction, ⟨11⟩, of the displacements. (b) Reconstruction associated with the low-coverage phase, e.g., $\Theta\approx 0.3$. The hydrogen atoms H have now polarized the W lattice in the ⟨10⟩ direction.

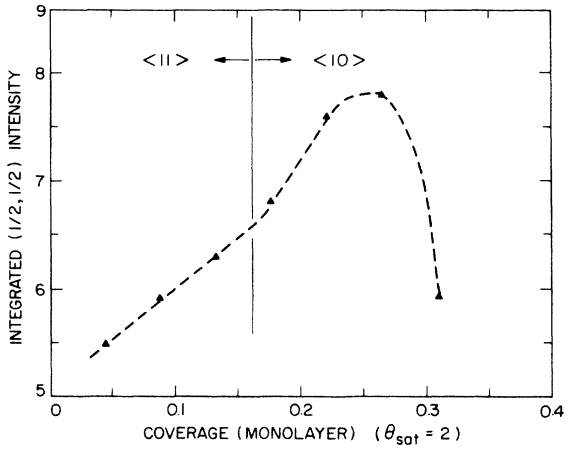

FIG. 3. Plot of the $(\frac{1}{2},\frac{1}{2})$ LEED spot intensity integrated over reciprocal space as a function of coverage determined according to Sec. IV E. The data were obtained with an OMA III (see text). The maximum integrated intensity occurs at $\Theta\approx 0.27$ which is well within the commensurate $(\sqrt{2}\times\sqrt{2})R45°$ phase. The intensity drops before the splitting becomes observable ($\Theta\approx 0.33$). The vertical line marks the point at which the W displacements are observed to switch from a ⟨11⟩ direction to a ⟨10⟩ direction by LEED (long-range probe).

ferent coverage calibration, Griffiths *et al.* observed the dip around $\Theta=0.1$. However, as discussed in Sec. IV E if the coverages are normalized at the point where the $(\frac{1}{2},\frac{1}{2})$ order spots split, then the two observations are well within the error bar.

The saturation coverage phase, characterized by a sharp (1×1) LEED pattern, has been well studied. The absolute coverage of $(2\pm0.2)\times10^{15}$ H atoms/cm^2, i.e., 2 H per W surface atom, has been measured by microanalysis[10,11] and no measurable lateral reconstruction (<0.05 Å) found by MeV ion channeling. Therefore, in agreement with LEED,[13,45,46] EELS,[38] and ir,[47,48] the surface is believed to be unreconstructed with all the hydrogen at the bridge site.

At lower coverages ($\Theta<0.5$), EELS has shown that hydrogen remains adsorbed at a bridge site because the normal modes (symmetric and asymmetric stretching modes and the wagging mode) associated with such a site could be observed.[12]

IV. RESULTS: INFRARED ABSORPTION

A. Overview

Figure 4 shows a summary of the infrared absorption data from $\Theta=0.04$ to $\Theta=0.88$, i.e., up to the $\frac{1}{5}$ order

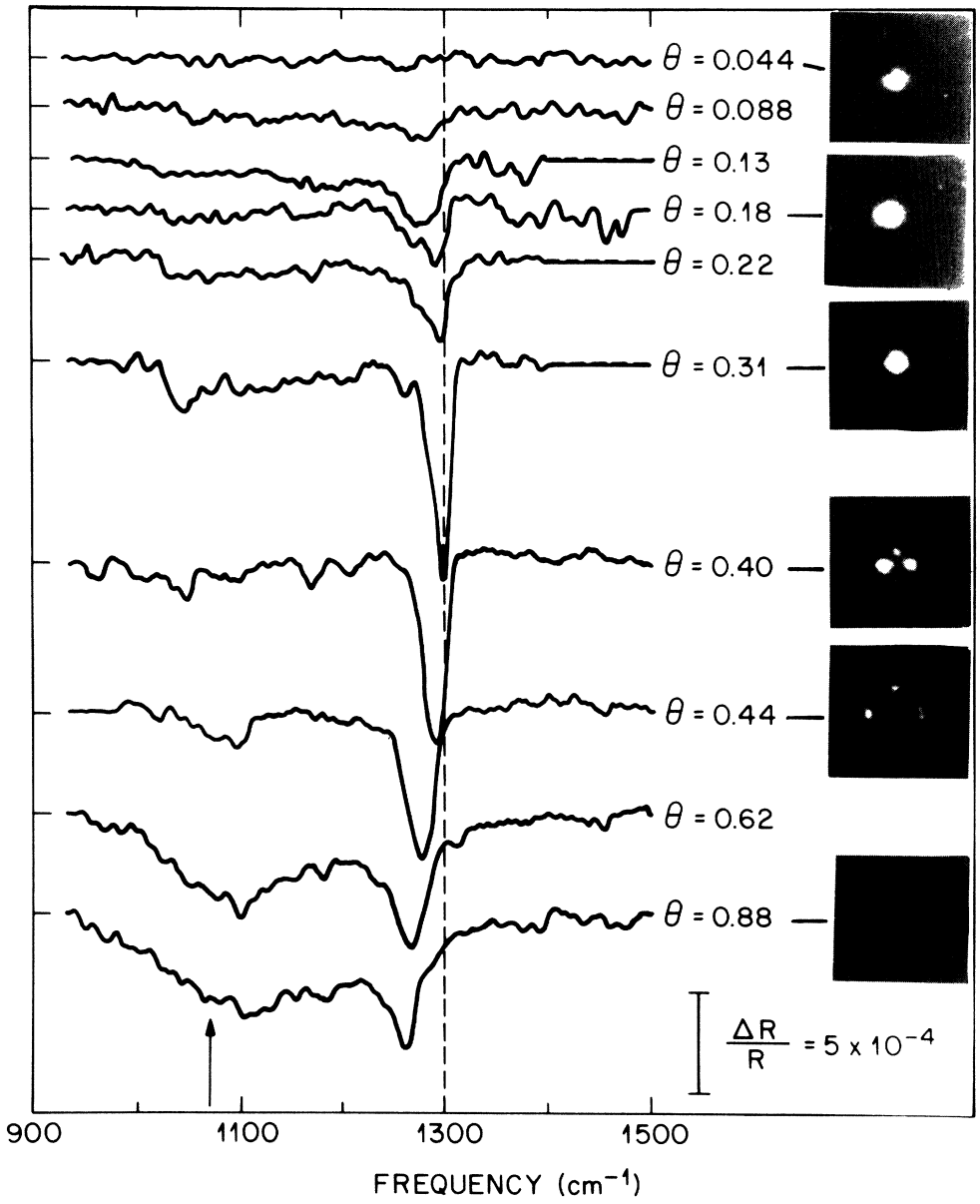

FIG. 4. ir spectra associated with H vibrations as a function of coverage and normalized as described in the text. The reference spectrum is that of the clean W(100) surface at room temperature. The $(\frac{1}{2},\frac{1}{2})$ LEED spot is shown for a few key coverages. The sharp feature at 1250–1300 cm^{-1} is associated with the ν_1 mode of H on pinched W (labeled ν_1' in the text). The vertical arrow shows the position of the ν_1 mode of H on unreconstructed W measured at saturation coverage (labeled ν_1 in the text). The resolution is 8 cm^{-1}.

reconstruction, and correlates such absorption to the LEED patterns. The region from $\Theta=0.88$ to $\Theta=2$ has been discussed in previous publications[47–49] and involves mainly the unreconstructed phase, with different degrees of order.

The data shown in Fig. 4 are obtained, in principle, by ratioing H-induced spectra with D-induced spectra, in order to remove any broadband absorption which is nonvibrational in nature. In practice, the broadband absorption is found to be linear in frequency over the range of interest (W_2H and W_2D vibrations)[47–49] so that a simple linear background subtraction can be performed.[50]

The resulting vibrational spectra show two major contributions, a relatively sharp absorption about 1300 cm^{-1} and a broader feature around 1100 cm^{-1} which we label ν_1' and ν_1, respectively, for the sake of brevity. As the coverage is increased, ν_1 grows relative to ν_1'.

At very low coverages ($\Theta \lesssim 0.31$) only ν_1' is present and is seen to shift up in frequency. At $\Theta=0.31$, ν_1 begins to appear and grows with coverage, while ν_1' broadens and shifts down in frequency. In Secs. IV B and IV C we consider these changes in detail.

B. Low coverage ($\Theta \lesssim 0.3$)

Figure 5 shows the peak position of ν_1' as a function of coverage. Note that the ν_1 contribution which appears at $\Theta=0.31$ is not considered in this plot. The error bars give the range of values measured for different runs, typically 4 or 5; thus they include the error associated with coverage determination. The vertical dashed line at $\Theta=0.16$ marks the point at which an inflection is seen in the $(\frac{1}{2},\frac{1}{2})$ LEED intensity, i.e., where the long-range order switches from a $\langle 11\rangle$ to a $\langle 10\rangle$ reconstruction (Fig. 2). As can be seen in Fig. 4, a definite shift in frequency occurs between $\Theta=0.13$ and $\Theta=0.18$. The data in Fig. 5 suggest that an inflection may also be present in the wave-number curve at $\Theta=0.16$ although the amplitude of such inflection is within the uncertainty of the data.

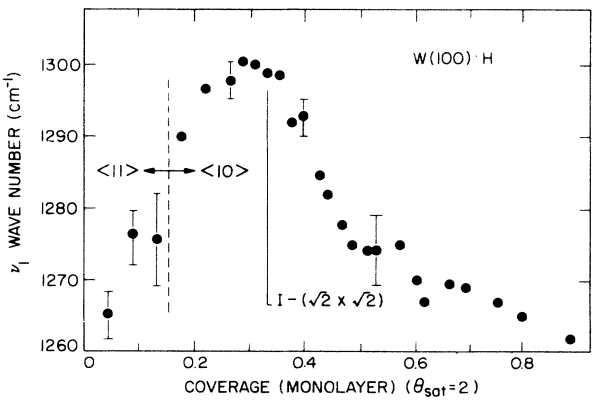

FIG. 5. Peak position (wave number) of the ν_1 mode (ν_1') as a function of coverage. For $\Theta > 1.0$, the ν_1 mode associated with H on pinched W (ν_1') is not observable and the ν_1 mode associated with H on unreconstructed W dominates the spectrum. The points at which the LEED data indicate a symmetry switch ($\Theta \approx 0.16$) and the beginning of the incommensurate phase ($\Theta \approx 0.33$) are indicated by dashed and solid lines, respectively.

The unambiguous part of the data is that the frequency of ν_1' increases $\gtrsim 35$ cm^{-1} from the isolated H limit ($\nu_1=1260$ cm^{-1}) to $\Theta=0.31$ ($\nu_1=1300$ cm^{-1}). This observation does not support the EELS data of Willis,[39] which suggested that the symmetric stretch remained at a fixed frequency for $\Theta < 0.4$.

The other observation is that, for the commensurate $(\sqrt{2}\times\sqrt{2})R45°$ phase at $\Theta \approx 0.3$, the frequency of ν_1' reaches a maximum (1300 cm^{-1}) and the linewidth a minimum (15 cm^{-1}). The observation of a lower frequency by EELS (155 meV = 1250 cm^{-1}) for this commensurate phase[12,39] is probably due to the superposition of both the ν_1 (1070 cm^{-1}) and the ν_1' (1300 cm^{-1}) as can be seen in Fig. 4 ($\Theta=0.31$). Note that higher resolution EELS data gave a peak at 159 meV (= 1282 cm^{-1}) (Ref. 37) at that coverage.

C. The incommensurate phase ($0.3 < \Theta \lesssim 0.5$)

In the range $\Theta=0.33$ to 0.42 the $(\frac{1}{2},\frac{1}{2})$-order LEED beam is split without any streaking. The splitting is first visible at $\Theta=0.33$ (see bottom left inset of Fig. 6) and increases continuously with coverage.[51] Figure 6 shows that dramatic shifts in vibrational frequency can be correlated to the splitting of the $(\frac{1}{2},\frac{1}{2})$-order LEED spot. Note that, in order to improve S/N, the *ratios* of H-spectra to the $\Theta=0.33$ spectrum are plotted. A shift in frequency therefore appears as a derivative-looking feature. Beside the shift of ν_1' towards lower frequencies with coverage, an increase of ν_1 (≈ 1100 cm^{-1}) is also apparent (vertical arrow, Fig. 6). However, as may be more clear in Fig. 4 ($\Theta=0.31$ to 0.44), the absorption increases by broadening ν_1 toward the high-frequency side. That is, except for the lowest detectable coverage ($\Theta=0.31$), ν_1 is quite broad, indicative of a broad distribution of W positions around the unreconstructed position.

The width of the ν_1' mode also increases as is shown more explicitly in Fig. 7. From a minimum of 15 cm^{-1} at $\Theta=0.31$ (commensurate phase) it increases to ≈ 22 cm^{-1} at $\Theta=0.41$ (incommensurate phase before streaking occurs). Although the half width at half maximum, $\Delta_{1/2}=11$ cm^{-1}, is of the same order as the shift (≈ 10 cm^{-1}), the high-frequency edge of the absorption clearly shifts down with coverage. This indicates that the mode broadens on the low-frequency side of the band. Finally, as the split spot begins to streak, ν_1' continues shifting down in frequency without further broadening [Fig. 7(e)].

D. The high-coverage phase ($\Theta > 0.5$)

Above $\Theta=0.5$, the ν_1' absorption decreases with coverage and is completely gone by $\Theta \approx 1.0$. The ν_1 contribution grows in strength and is very broad by $\Theta \approx 1.0$ [full width at half maximum (FWHM) ≈ 200 cm^{-1}]. In addition, as has been previously described,[48] the overtone of the wagging mode begins to contribute to the spectrum (≈ 1270 cm^{-1}) at $\Theta=0.6$. As a result, the infrared spectrum is complex and little spectral discrimination can be performed. However, the total integrated area of the spectrum contains useful information.

In Fig. 8 the integrated absorbance is plotted as a func-

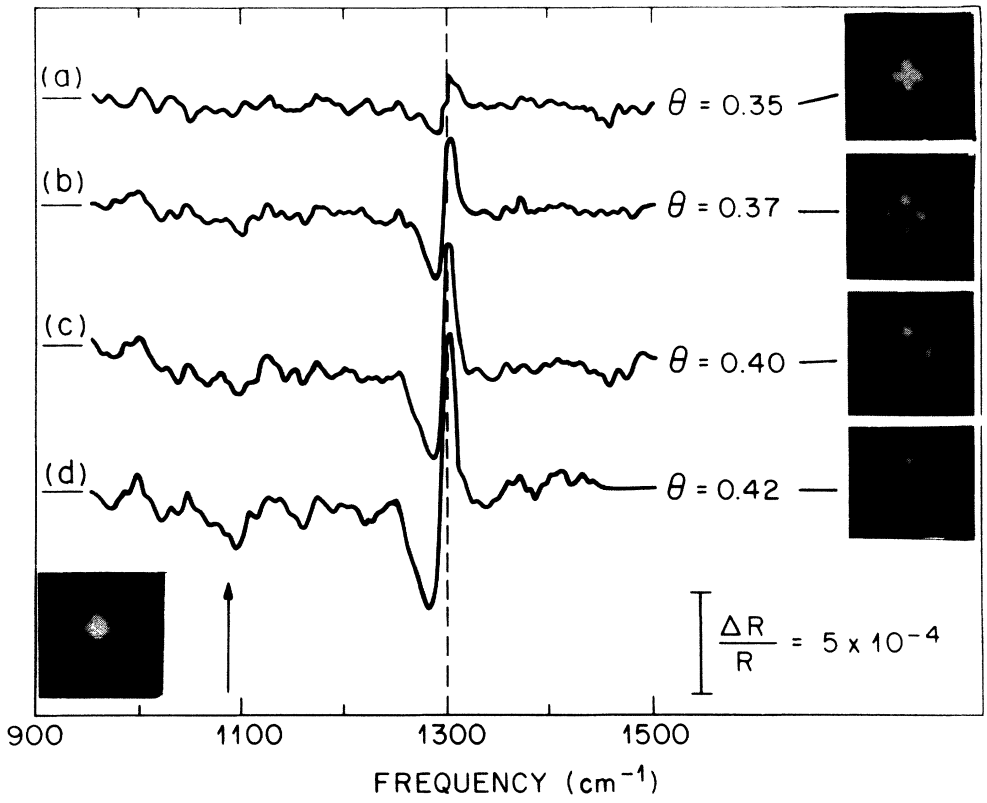

FIG. 6. Plot of the *relative* changes occurring in the spectra in the I-$(\sqrt{2}\times\sqrt{2})$ phase, i.e., between $\Theta=0.33$ and $\Theta=0.42$, with associated LEED pictures of the $(\frac{1}{2},\frac{1}{2})$ spot. All the spectra, from $\Theta=0.35$ to $\Theta=0.42$, are *ratioed* to that at $\Theta=0.33$ for which the $(\frac{1}{2},\frac{1}{2})$ LEED pattern is shown at the bottom left of the figure. (This reference is thus the surface for which the splitting begins to be observable.) A derivative looking feature indicates a shift in the absorption band. The resolution is 8 cm^{-1}.

tion of exposure. For $\Theta<0.6$, the integrated absorbance is linear with exposure. In this range the spectrum includes the symmetric stretch absorption only and is dominated by ν_1'. At saturation, the overtone absorption is sharp[47] and its contribution[52] can be taken out. The remaining area associated with the ν_1 mode *only* is shown by an open triangle.[53]

E. Coverage calibration and effective charge

For reasons given in Sec. II, we cannot determine the absolute coverage accurately in this experiment. In this section, we explain how the absolute coverage was established at $\Theta=0.33$ from the literature and how small relative changes could be measured for $\Theta<0.6$.

From Fig. 8 it appears that the ir absorbance for $\Theta<0.6$ is linear with exposure which in turn has been shown to be linear with coverage.[13,15,54] We can therefore use both the absorbance and exposure to measure small coverage changes ($\Delta\Theta\approx0.01$) in this range. In order to get an absolute coverage marker in this region, we use the point at which the $(\frac{1}{2},\frac{1}{2})$ LEED spot begins to split. According to King and Thomas,[13] this occurs at $\Theta\approx0.28$, while Barker and Estrup[15] found that $\Theta=0.37$ correspond to the coverage at which the splitting begins at room temperature. The latter also show that temperature affects this critical coverage. We therefore tentatively take this critical coverage to be $\Theta=0.33$, the average of these two values. Very recently, Riffe *et al.*[55] have determined using thermal desorption that the coverage for which the ir broadband absorptivity is smallest at room temperature is $\Theta=0.42\pm0.04$. At that coverage they observe the largest splitting of the $(\frac{1}{2},\frac{1}{2})$ LEED spot *without any streaking.* From our measurements at room temperature we find that the broadband absorptivity is smallest for the spectrum in Fig. 6(c). If $\Theta\approx0.4$ for Fig. 6(c), then $\Theta\approx0.33$ for the reference spectrum, the LEED pattern of which is shown in the bottom left inset of Fig. 6.

Thus, in this paper we have assigned the coverage at which the $(\frac{1}{2},\frac{1}{2})$ LEED spots begin to split to be $\Theta=0.33$, corresponding to a 0.375 L (1 L $=10^{-6}$ Torr sec) (under the experimental conditions described in Sec. II). For this coverage, the integrated ir absorbance is 1.3×10^{-2} cm^{-1} as shown in Fig. 8.

Keeping in mind that, while the relative coverage can be measured within 1%, the uncertainty in the *absolute* coverage is large, $\Delta\Theta=\pm0.4$ ($\Theta_{sat}=2$), the strength of the measured absorption can now be determined as a function of coverage. This absorption is not linear with coverage since, based on the value obtained at $\Theta=0.33$, a linear

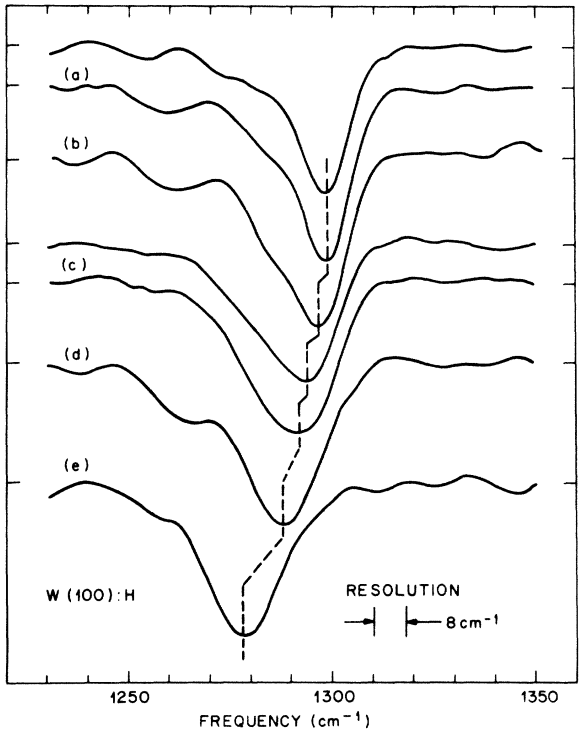

FIG. 7. ir spectra of the ν_1 mode associated with pinched W (ν_1') as a function of coverage, referenced to the *clean* W(100) surface at room temperature. The coverages, determined according to Sec. IV E, are (a) top: 0.30, bottom: 0.31; (b) 0.35; (c) top: 0.39, bottom: 0.40; (d) 0.41; (e) 0.48. The $(\frac{1}{2},\frac{1}{2})$ LEED spot is split *and* streaked at $\Theta=0.48$. (Saturation coverage is $\Theta=2$.)

dependence would give an integrated absorbance of 7.9×10^{-2} cm^{-1} at saturation ($\Theta=2$) instead of the measured 4.1×10^{-2} cm^{-1} (open triangle, Fig. 8).

A departure from linearity may arise because of a change in force constant or because of the electronic screening of the vibrator. The former is only weakly dependent on coverage and arises mostly from different bonding configurations. The latter only depends on coverage and will always be present independent of structural rearrangement.[56–58] Both effects are expected to be important in the case of H on W(100) because (a) the tungsten undergoes a large structural change in going from a pinched to an unreconstructed geometry and (b) the H density at saturation is high which will maximize the effects of screening.

Limiting values can be obtained for the sake of argument. For a dominant force constant mechanism, a decrease by approximately $\sqrt{2}$ in force constant for the unreconstructed structure can account for the data. On the other hand, if only screening were important as was assumed for the case of H on Pd(100) by Nyberg and Tengstäl,[59] then an electronic polarizability, $\alpha_e\approx0.7$ Å^3, is required.

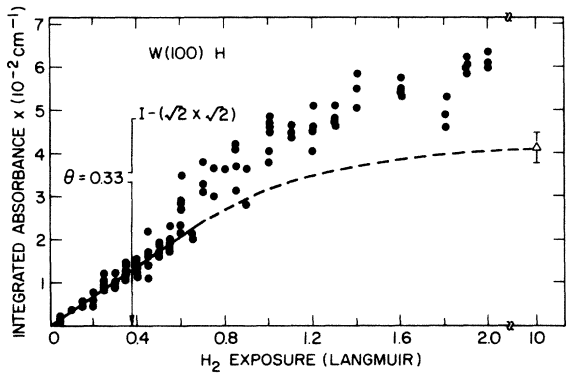

FIG. 8. Plot of integrated absorbance, $A\equiv-\log_{10}(1-\Delta R/R)$ as a function of exposure (1 L$=10^{-6}$ Torr sec). Calibration of the coverage is made by noting that the 1-$(\sqrt{2}\times\sqrt{2})$ phase starts at $\Theta=0.33$ as indicated. The straight line from 0 to 0.7 L results from a least-squares fit (linear regression) of all data points up to 0.7 L exposure (slope 3.5×10^{-2} cm^{-1}/L, correlation $=0.88$). The open triangle is the area associated with the ν_1 mode alone at saturation.

V. DISCUSSION

A. Mode assignment

Before a reliable mode assignment is performed, one must argue that a local picture, with simple central force constant is appropriate. Indeed, for H on some close packed surfaces, e.g., Ni(100) and Ni(111), it has been suggested[60] that the vibrational spectrum could be dominated by quantum effects. However, the fact that the W(100) surface is an open lattice which gets polarized by the H at low coverage,[13] and displays vibrational modes which can be assigned to a well-defined adsorption site (point-group symmetry), supports the nonquantum localized picture. Furthermore, at saturation coverage, the modes keep their respective assignment and the symmetric stretch broadens, instead of the expected sharpening if delocalization were important.[60]

Since H is adsorbed at a bridge site at all coverages, there are three nondegenerate vibrational modes characterizing the W_2H complex: the symmetric stretch (ν_1), the asymmetric stretch (ν_3), and the out of plane bend or wag (ν_2). For a symmetric dimer (not tilted), symmetry considerations dictate that, of the fundamental modes, only the symmetric stretch is infrared active. However, the overtones of the totally symmetric wag and asymmetric stretch are also allowed and may be detected under favorable conditions. The general consensus in the literature is that the frequency of the ν_1 mode increases as the W-W dimer distance decreases. There is, however, some controversy as to the behavior of the asymmetric stretch which we first discuss.

At saturation coverage, recent high-resolution EELS (Ref. 41) and ir (Ref. 47) data have suggested that the mode at ~1280 cm^{-1} (160 meV), originally assigned to the asymmetric stretch (Refs. 38 and 39), is in fact the overtone of the wagging mode (Ref. 48), located at ~645 cm^{-1} (80 meV). The asymmetric mode appears to be resolved at ~950 cm^{-1} (118 meV).[41] For the low-coverage phase, however, the early assignment of Barnes and Willis[12] for the asymmetric stretch at ~1010 cm^{-1} (125 meV) seems unambiguous. The intensity of this mode is stronger than that of the ν_2 mode at ~480 cm^{-1}

(60 meV) and does not occur at twice the frequency. It cannot therefore be the overtone of the wagging mode. Furthermore, the 1010 cm^{-1} (125 meV) loss is sufficiently removed from the ν_1 loss at saturation (132 meV) and displays enough nondipole, impact character that it cannot be assigned to the ν_1 mode on relaxed W domains at that coverage.

If the asymmetric stretch indeed varies from ~ 1010 cm^{-1} for the low coverage to ~ 950 cm^{-1} for the high-saturation phases then the accepted picture of a significant change in the W_2H bond angle between the two phases does not account for this new data. This picture is based on the assumption that simple W-H force constants (central forces only) can account for all three normal modes. Such an assumption may be inappropriate for an H at a bridge site for which the symmetric stretch is coupled to first order with bond-bending forces, while the asymmetric stretch is not. As a result, a stronger restoring force could be expected for the symmetric stretch than for the asymmetric stretch. However, very recent self-consistent slab calculations,[61] which reproduce well the vibrational frequency of the ν_1 and ν_2 mode at saturation coverage, find that the asymmetric stretch ν_3 is located around 1300 cm^{-1}. These calculations therefore support the simple central force picture for H on W(100).

For the purpose of interpreting the present ir data of the low-coverage mixed phases, it is sufficient to note that the asymmetric stretch mode cannot be detected at low coverage, i.e., there is no detectable absorption in the range 900 to 1030 cm^{-1} for $\Theta < 0.6$. Furthermore, since the surface is unreconstructed at saturation coverage the asymmetric stretch is ir forbidden by symmetry.[47] In the region of intermediate coverage, however, it is not possible to rule out a possible ν_3 absorption in the 1100 to 1200 cm^{-1} range arising from the presence of tilted dimers.[62–64] However, up to $\Theta = 0.6$ the linearity of absorbance versus exposure (Fig. 8) suggests that any ν_3 absorption is negligible.

The weak absorption around 1100 cm^{-1} at low coverage ($\Theta \lesssim 0.6$) is assigned to the symmetric stretch associated with W_2H in relaxed domains since it cannot be the overtone of the wagging mode or the asymmetric stretch.[12] We note, in particular that, since the ν_3 mode is not detectable in this range, it is unlikely that a large tilting of the W_2H complex occurs until the surface is well into the two-dimensional disordered phase characterized by a streaked $(\frac{1}{2},\frac{1}{2})$ LEED spot. The infrared measurements can therefore be used, for $\Theta \lesssim 0.6$, to obtain structural information on the W local reconstruction. In the 1100-cm^{-1} region, the absorption is associated with the symmetric stretch of H adsorbed on unreconstructed (relaxed) W. In the 1250- to 1300-cm^{-1} region, the absorption is associated with the symmetric stretch of H on pinched W.

B. Low coverage ($\Theta \lesssim 0.3$)

The only vibrational spectroscopic data available so far[39] have indicated that there was no frequency variation of the ν_1 mode from $\Theta = 0.15$ to $\Theta = 0.35$. And yet, several theoretical modelings of the low-coverage region including the symmetry switching and the commensurate $(\sqrt{2}\times\sqrt{2})R\,45°$ phase have predicted an increase in frequency with coverage.[28,29] The ir data presented in Fig. 5 are therefore particularly important in understanding the nature of the low-coverage phase.

Roelofs and Ying[25–28] have treated the H covered surface by combining a lattice-dynamic calculation for the clean W surface *and* a H lattice gas, performed within the mean-field approximation. This approach is particularly accurate for the low-coverage limit since it is based on an expansion in Θ. The model can reproduce the phase diagram determined by LEED studies,[15] thus making it possible to determine some of the interaction constants by using the experimentally determined dependence on temperature of the transition temperatures. In particular, they find that the energy difference between distortions along the $\langle 11\rangle$ and $\langle 10\rangle$ directions is 3 meV/atom in favor of the former for the *clean* surface. Furthermore, they find that the force representing the H-W interaction with respect to a motion parallel to the surface[28] is 0.2 eV/Å. As a result, they can account for the switch in symmetry of the long-range distortion at a low coverage.

Using a purely phenomenological approach based on the computation of the Ginzburg-Landau free energy for the clean surface and the introduction of a dominant H-W interaction through perturbation theory, Inaoka and Yoshimori[29] have determined the interaction parameters by fitting the thermal desorption data. Using the same parameters they then calculated the frequency dependence on coverage of the ν_1 mode. Defining $\tilde{\nu}_{\rm comm}$ the ν_1 frequency at $\Theta \approx 0.3$, $\tilde{\nu}_{\rm isolated}$ the ν_1 frequency at very low coverage ($\Theta \approx 0.04$), and $\tilde{\nu}_{\rm unreconst}$ the ν_1 frequency at $\Theta = 2$, they find that

$$(\tilde{\nu}^2_{\rm comm} - \tilde{\nu}^2_{\rm isolated})/(\tilde{\nu}^2_{\rm comm} - \tilde{\nu}^2_{\rm unreconst}) \approx 0.4$$

which is a factor of 2 larger than what the present measurements give.

A local microscopic picture, as pointed out by Heine,[65] would require that an isolated H atom, upon adsorption at a bridge site, pinch a pair of W atoms in the $\langle 10\rangle$ direction.[64] Since a displacement along the $\langle 10\rangle$ direction characterizes the very stable pinched phase $(\sqrt{2}\times\sqrt{2})R\,45°$ at $\Theta = 0.3$, it is expected that the same local displacement will exist at very low coverages (isolated H limit). While the clean surface features a $\langle 11\rangle$ displacement mostly due to the position of the second layer W atoms, the lowering in energy associated with H pinching the W atoms along the $\langle 10\rangle$ direction must be larger than ≈ 3 meV.

The increase of frequency of the ν_1 mode observed in Fig. 5 was therefore predicted qualitatively by the above theories. The picture which emerges is that the H polarizes locally the W along the $\langle 10\rangle$ direction. The vibrational frequency depends on the amplitude of displacement, which itself is a function of the coverage. Therefore, in order to use the ir results of Fig. 4 to gain *quantitative* information about interaction parameters, a knowledge of the W displacements is required.

As discussed in Sec. V A, interpretation of the EELS data based on comparison of the ratio $\tilde{\nu}_{\rm asym}/\tilde{\nu}_{\rm symm}$ (within a simple central force constant framework) with that for

bridge metal hydrides[12,39,40] may not be relied on to obtain accurate quantitative geometrical information. The most direct experiment to date which gives quantitative information on the lateral displacement is high-energy ion backscattering-channeling.[10,11] Although an energy dependence of the data for the $(\sqrt{2}\times\sqrt{2})R45°$ H-stabilized surface was not performed,[66] the value of the surface peak intensity for that phase combined with the energy dependence analysis of the clean W(100) surface indicates that half of the surface W atom is displaced by ≈ 0.2 Å.

Early LEED *I-V* data analysis suggested that the lateral motion of the W atoms could be between 0.15 and 0.3 Å, both for the clean surface and the H-covered $c(2\times2)$ surface. We note that an upper limit on the W displacement can be set by requiring that the W atoms along the $\langle 10\rangle$ direction be no closer than the nearest-neighbor bulk distance, $d=2.74$ Å. For a symmetrical W motion, the displacement should therefore be less or equal to 0.21 Å.

The ir data presented here suggest that a determination of the lateral displacement using Rutherford backscattering (RBS) may be quite difficult because the surface is not homogeneous: at very low coverages, the local W distortion in the immediate vicinity of the H atom is along the $\langle 10\rangle$ direction while large portions of the surface retain the $\langle 11\rangle$ displacement arrangement. Then as early as $\Theta=0.31$, a small portion of the surface is in a "relaxed" unreconstructed configuration, evidenced by the ν_1 contribution at 1070 cm^{-1} in Fig. 4 ($\Theta=0.31$). If indeed the clean surface reconstruction does not involve displacement of a full monolayer then no noticeable changes in the value of surface peak intensity would be expected as H is adsorbed, *even if locally both W atoms are pinched symmetrically about H by as much as 0.21* Å. Thus, at no coverage can ion scattering detect a full monolayer of W atoms displayed by the *same* amount. Therefore, since a lower limit on the displacement was set at 0.2 Å (600-keV ions data), it is reasonable to assume that the local rearrangement of *each* pinched W at low coverage ($\Theta\approx0.3$) is ≈ 0.2 Å.

Assuming that the frequency of the ν_1 mode is proportional to the W-W dimer distance,[67] we can use the present data to estimate the lateral W motion occurring in going from the isolated H limit to the commensurate $(\sqrt{2}\times\sqrt{2})R45°$ domain. From the frequency corresponding to the unreconstructed saturation phase (1070 cm^{-1}) and the fully reconstructed phase (1300 cm^{-1}), we deduce that, in the isolated case ($\tilde{\nu}\approx1260$ cm^{-1}), the W dimer length is 0.07 Å larger than at $\Theta=0.3$. That is, an isolated H will polarize each neighboring W atom by ≈ 0.16 Å from their unreconstructed position instead of 0.2 Å at $\Theta\approx0.3$.

Combining the estimates of the change in dimer length given above and that of the polarizing force associated with a parallel motion derived by Roelofs and Ying,[28] an estimate of the energy associated with the change in the local distortion around an isolated H ($\Theta<0.1$) can be obtained. That energy is: 0.2 eV/Å $\times$ 0.035 Å $=7$ meV.

Thus, within the above stated assumptions, the energy associated with the strain field around an isolated pinched W_2H moiety on the W(100) surface can be estimated from the measured frequency shift. The associated energy can be used directly to determine the change in the coverage dependent activation energy in the low-coverage region and to check it against the absolute estimates obtained from the fitting of thermal-desorption experiments.[29] We also note that 7 meV corresponds to an energy close to that associated with the change in ir transition (≈5 meV). Such information will be useful when the details of the potential well for the reconstructed surface are uncovered by self-consistent slab calculations.

C. The incommensurate phase ($0.3<\Theta<0.5$)

As first worked out by Fujiwara[68] and later generalized by Houston and Parks,[69] continuous LEED beam splitting arises when the mean in the distribution of domain size changes continuously as a function of some parameters, e.g., coverage, and the domains are in registry with the underlying lattice. The resulting phase is called incommensurate because the modulation wavelength of the domain size in general *incommensurate* with the lattice.

The modulation wavelength and the width of the distribution can be obtained from LEED. However, LEED does not give any information on the nature of the boundary region (wall) between the reconstructed domains. Such information is critical to decipher between various mechanisms proposed to explain the transition to an incommensurate phase.

Fasolino *et al.*[23] have proposed that the incommensurate phase arises from the coupling of two vibrational modes, one perpendicular to and the other in the plane of the surface. Such a coupling would be maximum at the boundary between domains and represents a special case of the general mechanism proposed by Heine and McDonnel for the incommensurate phase in ferroelectrics.[70] The incommensurate state is represented by a sinusoidal state with a single incommensurate wave vector, leading to a mode distribution of local arrangements and no sharp boundaries between the domains.

Ying and Hu have shown that such a sinusoidal variation overestimates the energy of the incommensurate state and leads to a first-order $C\rightarrow I$ transition.[71] Using a microscopic lattice-dynamic Hamiltonian approach, they derived a "soliton" Hamiltonian which described the incommensurate phase, not by a sinusoidal displacement of a single incommensurate wave vector, but rather by a periodic structure of antiphase domain walls (solitons) separating commensurate regions. Such soliton models account well for the transitions in physisorption systems and transition-metal dichalcogenides,[72] and had been suggested by Willis for the H/W(100) system.[73]

More recently, Heine[65] has suggested that a "split soliton" picture, in which the reconstructed domains are separated by a finite and well-defined unreconstructed region (plateau) need to be invoked to account for the infrared data. In both the Willis and Heine model, the H atoms are thought to adsorb preferentially on the reconstructed domains (higher binding energy) and only fill the less reconstructed (more relaxed) wall regions *after* the domains are full.

The data shown in Fig. 4 for $\Theta=0.31$ and a quantita-

tive analysis of the area under ν_1' for the data of Fig. 6 show that H on unreconstructed, relaxed W ($\nu_1 \approx 1100$ cm^{-1}) can be detected *before* the integrated intensity under ν_1' starts to decrease ($\Theta \approx 0.41$). Although careful thermal-desorption studies[16] have shown that the binding energy of H on unreconstructed W sites ($E \approx 17$ KCal/mole) is smaller than that of H on reconstructed W sites ($E \approx 40$ KCal/mole), the situation in the incommensurate phase appears more complex. The wall regions, which are believed to be mostly unreconstructed, *can* accommodate H atoms *before* the $c(2\times2)$ domains are saturated at room temperature.

A direct result of the data, irrespective of the local binding energy of H at domain walls, is the fact that these domain-wall areas have a finite width. Antiphase domains with zero-width domain walls, schematically illustrated by Barker and Estrup,[15] can be ruled out. Although the width of the domain walls is expected to increase with coverage, the data cannot give a quantitative estimate of a width change. However, the total area occupied by the *reconstructed* domains decreases as the number of domains and domain walls increases,[74] as expected in the soliton picture.

As the domain size decreases, ν_1' and ν_1 shift and broaden toward high and low frequency, respectively (Figs. 6 and 7), indicating that the modulation of the W displacement is increased. By the time the split spots streak [Fig. 7(e)], ν_1' continues to shift down in frequency without further broadening. Hence, if the broadening is associated with W-W dimer length modulation, then the formation of smaller domains along the perpendicular direction (i.e., domain walls are parallel to the W-W dimer direction) as evidenced by the direction of the streaking does not affect the ir linewidths. This observation is consistent with a model where the domain walls are first perpendicular to the substrate atom displacements. In contrast, the streaking which is induced by steps occurs along the same direction as that induced by higher coverages of hydrogen, which indicates that the step edges are parallel to the substrate atom displacements as suggested by Estrup[8,15] and Wendelken.[75]

VI. CONCLUSIONS

This high-resolution vibrational study of the symmetric stretch mode (ν_1) of H on W(100) at sub-saturation coverages ($0.04 \leq \Theta < 2$) has shown that (a) ν_1 undergoes a continuous frequency shift with coverage as the commensurate $(\sqrt{2}\times\sqrt{2})R45°$ phase is formed ($\Theta \approx 0.3$) and (b) the incommensurate phase is characterized by a domain structure with $(\sqrt{2}\times\sqrt{2})R45°$ symmetry separated by *finite-size* domain wall areas. This information, which was not available from previous EELS studies, makes it possible to eliminate some of the proposed models and to support some of the predictions for this system.

The continuous shift at low coverages ($\Theta < 0.3$) quantitatively support the calculations of Roelofs and Ying, and are qualitatively consistent with the calculation of Inaoka and Yoshimori and of Heine. The evidence for distinct domains with finite-size domain walls clearly rule out a *sinusoidal modulation* of the top-layer W displacements. It also rules out the formation of antiphase domains with *sharp* boundaries. Rather, it indicates that an intermediate picture, such as that described by the soliton or split soliton model, best accounts for the data.

Furthermore, the signal-to-noise ratio of these infrared experiments has made it possible to show that the adsorption energy for H on "unreconstructed" W at the domain walls is comparable with that of H on "pinched" W in the low-coverage regime. This knowledge, combined with the accurate measurements of frequency shifts at low coverages is complementary information to thermal-desorption studies and is critical to test the various phenomenological models.

Similar high-resolution studies over a wide range of temperatures are clearly needed to understand the phase transitions, particularly the $C \rightarrow I$ $(\sqrt{2}\times\sqrt{2})$ transition. At present, such studies are difficult because the reflectivity variations with temperature cannot be well ratioed out, due to thermal drifts in the sample manipulator. However, the signal-to-noise ratio ($S/N > 10^4$) obtained within short times (≈ 3 min) over a wide frequency range (650 to 5000 cm^{-1}) clearly shows the versatility of surface infrared spectroscopy for the *high-resolution* vibrational studies of adsorbates on metal surfaces.[76]

ACKNOWLEDGMENTS

The authors are grateful to D. R. Hamann, S.-C. Ying, V. Heine, A. Yoshimori, P. J. Estrup, and D. A. King for stimulating discussions and to E. E. Chaban for technical support. J.J.A. thanks AT&T Bell Laboratories for financial support.

*Present address: University of Illinois at Urbana-Champaign. Contact second author (Y.J.C.) for information.

[1]P. J. Estrup and J. Anderson, J. Chem. Phys. **45**, 2254 (1966).
[2]K. Yonehara and L. D. Schmidt, Surf. Sci. **25**, 238 (1971).
[3]T. E. Felter, R. A. Barker, and P. J. Estrup, Phys. Rev. Lett. **38**, 1138 (1977).
[4]M. K. Debe and D. A. King, J. Phys. C **10**, L303 (1977).
[5]M. K. Debe and D. A. King, Phys. Rev. Lett. **39**, 709 (1977).
[6]M. K. Debe and D. A. King, Surf. Sci. **81**, 193 (1979).
[7]J. A. Walker, M. K. Debe, and D. A. King, Surf. Sci. **104**, 405 (1981).
[8]R. A. Barker and P. J. Estrup, Phys. Rev. Lett. **41**, 1307 (1978).
[9]R. A. Barker, P. J. Estrup, F. Jona, and P. M. Marcus, Solid State Commun. **25**, 375 (1978).
[10]I. Stensgaard, L. C. Feldman, and P. J. Silverman, Phys. Rev. Lett. **42**, 247 (1979).
[11]L. C. Feldman, P. J. Silverman, and I. Stensgaard, Surf. Sci. **87**, 410 (1979).
[12]M. R. Barnes and R. F. Willis, Phys. Rev. Lett. **41**, 1729 (1978).
[13]D. A. King and G. Thomas, Surf. Sci. **92**, 201 (1980).
[14]P. J. Estrup, J. Vac. Sci. Technol. **16**, 635 (1979).
[15]R. A. Barker and P. J. Estrup, J. Chem. Phys. **74**, 1442 (1981).
[16]A. Horlacher Smith, R. A. Barker, and P. J. Estrup, Surf. Sci.

136, 327 (1984).
[17]J. C. Campuzano, J. E. Inglesfield, D. A. King, and G. Somerton, J. Phys. C **14**, 3099 (1981).
[18]M. I. Holmes and T. Gustafsson, Phys. Rev. Lett. **47**, 443 (1981).
[19]M. Posternak, H. Krakauer, and A. J. Freeman, Phys. Rev. B **25**, 755 (1982).
[20]D. W. Bullett and P. C. Stephenson, Solid State Commun. **45**, 47 (1983).
[21]I. Temkura, K. Terakura, and W. Hamada, Surf. Sci. **103**, 103 (1981); **111**, 479 (1981).
[22]C. L. Fu, A. J. Freeman, E. Wimmer, and M. Weinert, Phys. Rev. Lett. **54**, 2261 (1985).
[23]A. Fasolino, G. Santoro, and E. Tosatti, Phys. Rev. Lett. **44**, 1684 (1980); Surf. Sci. **125**, 317 (1983).
[24]K. H. Lau and S.-C. Ying, Phys. Rev. Lett. **44**, 1222 (1980).
[25]S.-C. Ying and L. D. Roelofs, Surf. Sci. **125**, 218 (1983).
[26]L. D. Roelofs, G.-Y. Hu, and S.-C. Ying, Phys. Rev. B **28**, 6369 (1983).
[27]L. D. Roelofs, G.-Y. Hu, and S.-C. Ying, J. Vac. Sci. Technol. A **2**, 894 (1984).
[28]L. D. Roelofs and S. C. Ying, Surf. Sci. **147**, 203 (1984).
[29]T. Inaoka and A. Yoshimori, Surf. Sci. **149**, 241 (1985).
[30]W. F. Engelhoff and D. L. Perry, Phys. Rev. Lett. **34**, 93 (1975).
[31]B. Feuerbacher and R. F. Willis, Phys. Rev. Lett. **36**, 1339 (1976).
[32]J. Anderson, G. J. Lapeyre, and R. J. Smith, Phys. Rev. B **17**, 2436 (1978).
[33]S.-L. Weng, E. W. Plummer, and T. Gustafson, Phys. Rev. B **18**, 1718 (1978).
[34]J. C. Campuzano, D. A. King, C. Somerton, and J. E. Inglesfield, Phys. Rev. Lett. **45**, 1649 (1980).
[35]D. E. Eastman, F. J. Himpsel, and J. F. VanderVeen, J. Vac. Sci. Technol. **20**, 609 (1982).
[36]C. Guillot, M. C. Desjongueres, D. Chauveau, and G. Treglia, Solid State Commun. **50**, 393 (1984).
[37]A. Adnot and J.-D. Carette, Phys. Rev. Lett. **39**, 209 (1977).
[38]W. Ho, R. F. Willis, and E. W. Plummer, Phys. Rev. Lett. **40**, 1463 (1978); R. F. Willis, W. Ho, and E. W. Plummer, Surf. Sci. **80**, 593 (1979).
[39]R. F. Willis, Surf. Sci. **89**, 457 (1979).
[40]U. A. Jayasooriya, M. A. Chesters, M. W. Howard, S. F. A. Kettle, D. B. Powell, and N. Sheppard, Surf. Sci. **93**, 526 (1980).
[41]J. P. Wood and J. L. Erskine, Phys. Rev. Lett. **55**, 2595 (1985).
[42]A description of the apparatus is given in Y. J. Chabal, E. E. Chaban, and S. B. Christman, J. Electron. Spectr. Rel. Phenom. **29**, 35 (1983), in E. E. Chaban and Y. J. Chabal, Rev. Sci. Instrum. **54**, 1031 (1983), and in Y. J. Chabal, G. S. Higashi, and S. B. Christman, Phys. Rev. **28**, 4472 (1983).
[43]See D. M. Riffe, L. M. Hanssen, A. J. Sievers, Y. J. Chabal, and S. B. Christman, Surf. Sci. **161**, L559 (1985); D. M. Riffe, L. M. Hanssen, and A. J. Sievers, Bull. Am. Phys. Soc. **30**, 361 (1985) and Phys. Rev. B (to be published).
[44]K. Griffiths, D. A. King, and G. Thomas, Vacuum **31**, 671 (1981).
[45]G.-C. Wang, J. Unguris, D. T. Pierce, and R. J. Celotta, Surf. Sci. **114**, L35 (1982); M. A. Passler, B. W. Lee, and A. Ignatiev, Surf. Sci. **150**, 263 (1985).
[46]See review by, D. A. King, Phys. Scr. T **4**, 34 (1983).
[47]Y. J. Chabal, Phys. Rev. Lett. **55**, 845 (1985).
[48]Y. J. Chabal, J. Vac. Sci. Technol. A **4**, 1324 (1986).
[49]Y. J. Chabal, in Proceedings of the Fourth International Conference on Vibrations at Surfaces, Lake District (England), 1985 [J. Electron Spectr. Rel. Phenom. **38**, 159 (1986)].
[50]Relative to the clean W(100) surface at room temperature, the background absorption varies substantially as a function of coverage. It first increases up to $\Theta=0.15$, then decreases substantially up to $\Theta\approx0.4$. As the $(\frac{1}{2},\frac{1}{2})$ spot streaks, the absorption increases precipitously to a level well above that of the clean surface, reaching a maximum at $\Theta\approx1.2$. From that point on, it slowly decreases but remains larger than for the clean W(100) surface. Although the power-law dependence on frequency is not exactly linear (see Ref. 43) it is weak enough that it can be well approximated by a straight line over the small frequency range (≈200 cm^{-1}) of interest.
[51]The value $\Theta=0.33$ is defined, see Sec. IV E.
[52]Its line shape is well fitted by the expression derived by D. C. Langreth, Phys. Rev. Lett. **54**, 126 (1985). See Ref. 47.
[53]The error bar arises mainly from the uncertainties in the background subtraction.
[54]T. E. Madey, Surf. Sci. **36**, 281 (1973).
[55]D. M. Riffe, L. M. Hanssen, and A. J. Sievers (unpublished).
[56]G. D. Mahan and A. A. Lucas, J. Chem. Phys. **68**, 1344 (1978).
[57]B. N. J. Persson and R. Ryberg, Phys. Rev. B **24**, 6954 (1981).
[58]S. Anderson and B. N. J. Persson, Phys. Rev. Lett. **45**, 1421 (1980).
[59]C. Nyberg and C. G. Tengstäl, Phys. Rev. Lett. **50**, 1680 (1983).
[60]M. J. Puska, R. M. Nieminen, M. Manninen, B. Chakraborty, S. Holloway, and J. K. Nørskov, Phys. Rev. Lett. **51**, 1081 (1983).
[61]R. Biswas and D. R. Hamann (unpublished).
[62]E. F. J. Didham, W. Allison, and R. F. Willis, Surf. Sci. **126**, 219 (1983).
[63]E. F. J. Didham, M. S. Foster, B. J. Hinch, and R. F. Willis, J. Phys. (Paris) Colloq. **45**, C5-113 (1984).
[64]R. F. Willis, in *The Structure of Surfaces,* Vol. 2 of *Springer Series in Surface Science,* edited by M. A. Van Hove and S. Y. Tong (Springer-Verlag, New York, 1985), p. 237.
[65]V. Heine (private communication).
[66]Such a measurement is not expected to yield results different from those of the clean surface.
[67]This assumption may not be valid if the force constant changes upon reconstruction. See Sec. IV E.
[68]K. Fujiwara, J. Phys. Soc. Jpn. **12**, 7 (1957).
[69]J. E. Houston and R. L. Park, Surf. Sci. **21**, 209 (1970).
[70]V. Heine and J. D. C. McConnell, J. Phys. C **17**, 1199 (1984); V. Heine, J. D. C. McConnell, Phys. Rev. Lett. **46**, 1092 (1981).
[71]S. C. Ying and G. Y. Hu, in *The Structure of Surfaces,* Ref. 64, p. 341.
[72]W. McMillan, V. L. Pokrovsky, and A. L. Talapov, Zh. Eksp. Teor. Fiz. **78**, 269 (1980) [Sov. Phys.—JETP **51**, 134 (1980)].
[73]R. F. Willis, in *Many Body Phenomena at Surfaces,* edited by D. Langreth and H. Suhl (Academic, New York, 1984), p. 297, and references therein.
[74]A more quantitative statement cannot be made because the adsorption energy of H on domain walls relative to that on terraces is not known.
[75]J. F. Wendelken and G.-C. Wang, J. Vac. Sci. Technol. A **3**, 1593 (1985).
[76]For recent developments in Surface Infrared Spectroscopy, see the Proceedings of the Fourth International Conference on Vibrations at Surfaces, [J. Electron Spectr. Rel. Phenom. **38** (1986)].

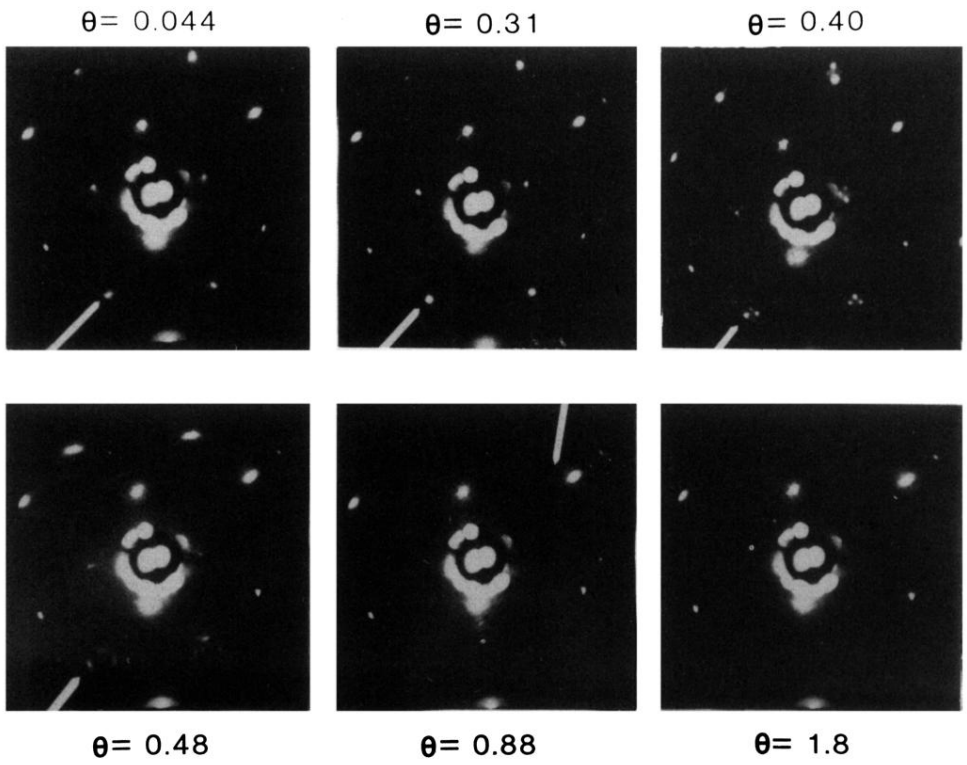

FIG. 1. Summary of the main stages of reconstruction as a function of coverage as monitored by LEED. For $\Theta=0.04$, 0.31, 0.40, and 0.48, the $(\frac{1}{2},\frac{1}{2})$ LEED spot is indicated by an arrow. The coverage is determined by ir absorbance and exposure (see Sec. IV E). For $\Theta\approx 0.88$, the weak $\frac{1}{5}$-order spot is marked. The coverages for the last two frames are estimated using ir absorbance and interpolation between $\Theta=0.6$ and $\Theta=2$.

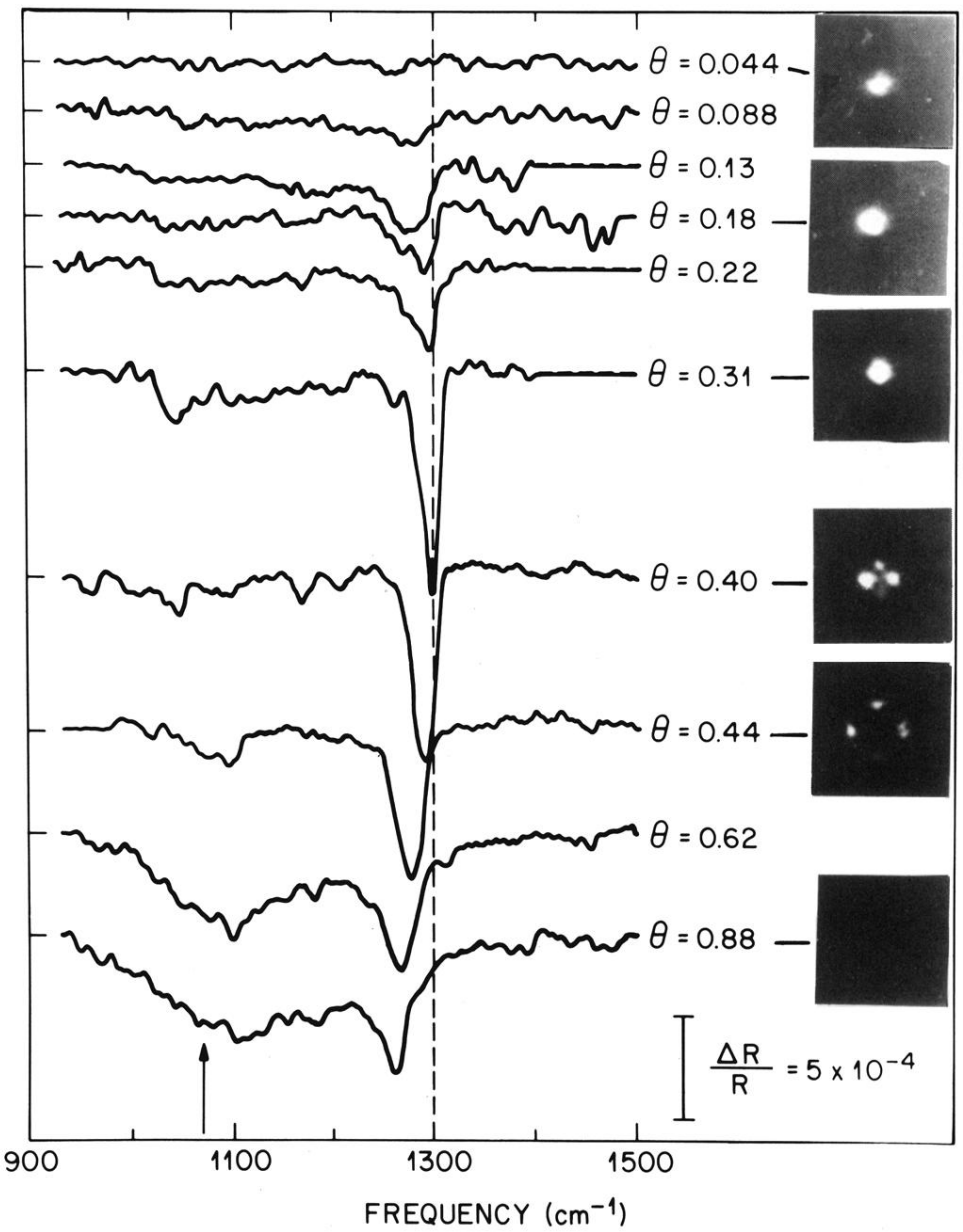

FIG. 4. ir spectra associated with H vibrations as a function of coverage and normalized as described in the text. The reference spectrum is that of the clean W(100) surface at room temperature. The $(\frac{1}{2},\frac{1}{2})$ LEED spot is shown for a few key coverages. The sharp feature at 1250–1300 cm^{-1} is associated with the ν_1 mode of H on pinched W (labeled ν_1' in the text). The vertical arrow shows the position of the ν_1 mode of H on unreconstructed W measured at saturation coverage (labeled ν_1 in the text). The resolution is 8 cm^{-1}.

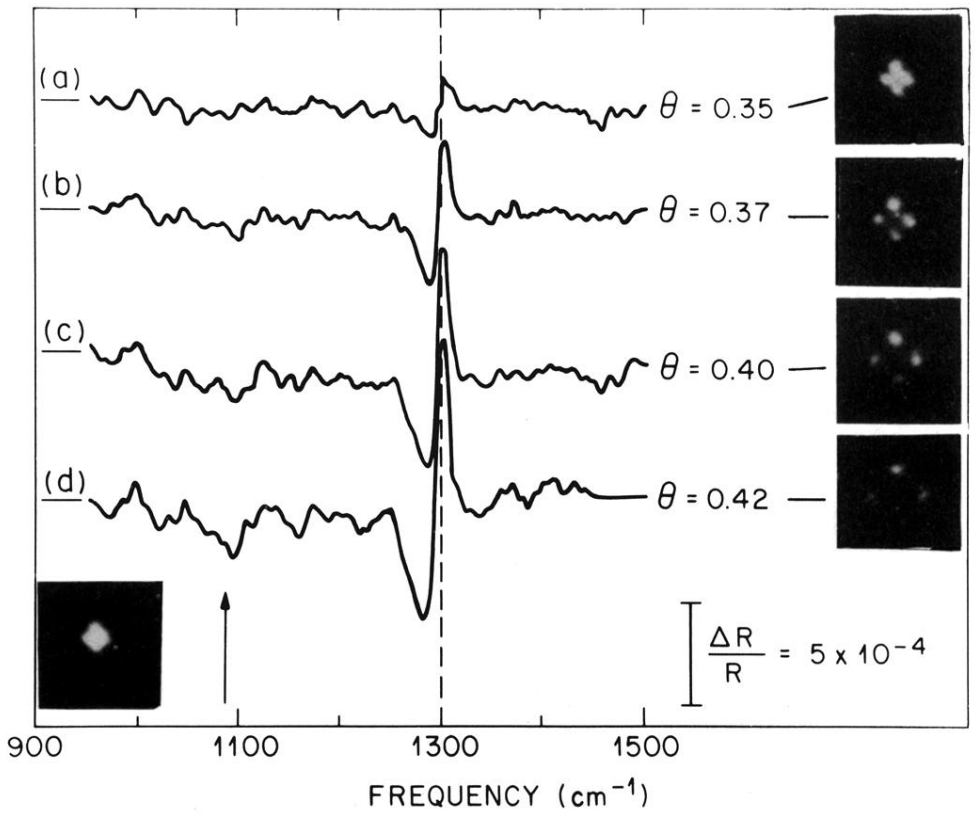

FIG. 6. Plot of the *relative* changes occurring in the spectra in the I-$(\sqrt{2}\times\sqrt{2})$ phase, i.e., between $\Theta=0.33$ and $\Theta=0.42$, with associated LEED pictures of the $(\frac{1}{2},\frac{1}{2})$ spot. All the spectra, from $\Theta=0.35$ to $\Theta=0.42$, are *ratioed* to that at $\Theta=0.33$ for which the $(\frac{1}{2},\frac{1}{2})$ LEED pattern is shown at the bottom left of the figure. (This reference is thus the surface for which the splitting begins to be observable.) A derivative looking feature indicates a shift in the absorption band. The resolution is 8 cm^{-1}.